Defence Science Journal, Vol. 61, No. 1, January 2011, pp. 12-18, DOI: 10.14429/dsj.61.163

Thermography for Performance Optimisation of Spark-ignition Engine due to Soot Formation in Exhaust Pipe

S.S. Singh and A.K. Singh*

Defence Institute of Advanced Technology, Pune–411 025
**Email: draksingh@hotmail.com*

ABSTARCT

The usage of thermography as an effective condition monitoring tool for performance evaluation on spark-ignition engine has been discussed. The technique allows for the monitoring of temperatures and thermal patterns while the equipment are running under loaded condition. The experiments have been conducted on petrol engine to acquire thermographs of the exhaust pipe under different loads with different diameters of the exhaust pipe to provide condition for soot formation. The heat transfer analysis was carried out using properties of CO_2 for three different flow areas by inserting metallic tubes of known thickness in the exhaust pipe. The paper emphasises that soot formation will reduce the flow area which will result in increase in the surface temperature and the thickness of soot layer can be further correlated with the running performance of the engine.

Keywords: Condition monitoring, infrared thermography, thermocouple, conduction, convection, internal gas temperature, thermal resistance

1. INTRODUCTION

Infrared (IR) thermography is being targeted as a versatile tool for condition monitoring of equipments[1,2]. Infrared imaging helps to quickly and efficiently find the areas maximum in need of maintenance. The infrared thermal imaging method utilises the radiations in the infrared spectral band from measured objects to measure temperature. It is non-intrusive, applicable remotely, and suitable for measurement[3] of a large area, and can also serve to record data for subsequent storage and further processing by a computer. Ay[4], *et al.* used an infrared thermal imaging camera to observe the surface temperature of a plate finned-tube heat exchanger and calculated the local heat transfer coefficient. The aim was to maintain the equipments by evaluating its performance at specific time intervals. IR thermography on equipments show the surface thermal patterns which are a consequence of internal conditions. Using heat transfer analysis[5], the internal conditions can be evaluated to show the external surface conditions.

The purpose of this study was to determine the applicability of IR thermography as a condition monitoring tool for spark-ignition engine and to draw an analogy between the operating condition and excessive soot formation in the exhaust manifold of the engine.

2. INSTRUMENTATION

A portable thermal imaging camera (EEV make, Model P 4430) was used to record thermal image of spark-ignition engine exhaust pipe. It incorporates a video output which can be used for direct thermal image recording to a computer. The P4430 is a hand-held thermal imaging camera with pyroelectric videocon detector having spectral response of 8-12 µm. It is a self-contained battery/ac power-operated unit incorporating a miniature display monitor and can be fitted with interchangeable lens (focal length 50/75 mm f 0.8 NOM lenses) and angle of view 17/11 deg, i.e., FOV, defined in combination with lens used. The equipment is for general thermal imaging applications and gives monochrome thermal pictures. The external video signal is 1 volt 625 lines 50 Hz (CCIR compatible) or 525 lines 60 Hz (optional), 30 frames/sec, and 200 lines per picture height for a temperature difference of 2 °C (chopped) and 1 °C (panned). A personal computer having Q motion card for image acquisition and WINVIDEO with Windows operating system has been used. An IR thermometer gun OPTEX THERMO-HUNTER make (Model Q185) was used for direct temperature reading of the object surface having provision of emissivity adjustment. The temperatures was measured using T type thermocouples. For this, a data acquisition (DA) system using GENIE software comprising ADAM 4018, with inbuilt signal conditioning for thermocouple input and analog-to-digital converter, and ADAM 4520, for interfacing ADAM-4018 with PC, data acquisition modules (M/S Advantech, USA), was used.

The camera was calibrated with a hot plate (top surface cast iron) having built-in heater and temperature controller and surface temperature was measured with *t* type thermocouples, placed on the top surface, and IR temperature gun for calibration and comparison purpose.

Recieved 22 December 2009, Revised 27 October 2010, Published Online 6 January 2011

The temperature scaling of the thermographs have been done by interpolating the gray scale value of the portion of the image to the temperature range, as obtained by the infrared thermometer.

3. EXPERIMENTS ON PETROL ENGINE

Experiments were carried out on a 0.2 l fuel-injected SI gasoline engine, Make Shriram Honda. Block schematic of experimental setup is shown in Fig. 1. Experimental tests were carried out at the engine test bench using infrared thermography. The exhaust gas temperature was measured at both the inlet and outlet of the exhaust pipe and an average value at different loads was taken for properties evaluation. The thermal images with different internal diameter at different loads are shown in Fig. 2. The thermography data made it possible to compare the surface temperature of the exhaust pipe at different engine loads with values calculated using the heat transfer theory. These calculations have been based on following assumptions. Largest component of the exhaust gases is assumed CO_2, hence the properties of carbon dioxide are used for exhaust flow analysis.The properties were interpolated based on equations as derived from the tabulated values.

4. EXHUAST GAS TEMPERATURE AND RATE MEASUREMENTS

The exhaust gas temperature was measured using thermocouple both at the inlet and the outlet of the exhaust pipe. The readings were taken for three different areas and an average estimation was made for properties evaluation. The calculated values are given in Table 1.

The exhaust flow rate was evaluated using following relation.

$$m_{exh} = m_{air} + m_{fuel} \tag{1}$$

For the air flow, the orifice method was used. The air entering the engine passes first through an orifice plate and the pressure drop across the orifice plate gives the measure of the air flow rate using the following relation:

$$m_{air} = C_a \times A_o \times (2 \times \Delta P \times \rho_{air})^{1/2} \tag{2}$$

where $C_d = 0.64$ (coefficient of discharge of orifice), $A_o = 0.00017671$ m^2 (area of orifice) and $\rho_{air} = 1.178$ kg/m^3 (density of air).

$$\Delta P = \rho_W \times \Delta H \times g \tag{3}$$

where $\rho_w = 1000$ kg/m^3, ΔH = Vertical difference in fluid levels (m), $g = 9.81$ m/s^2 (gravitational acceleration)

The fuel flow is measured using a pipette of 100 ml capacity. The fuel flow rate is calculated using following relation:

$$m_{fuel} = (V_f / t) \times (\rho_{fuel} / 10^6) \tag{4}$$

where, V_f = fuel (ml), ρ_{fuel} = density of fuel (780 kg/m^3), and t = time (s). The various flow rates for different loads is tabulated in Table 2 using above relations.

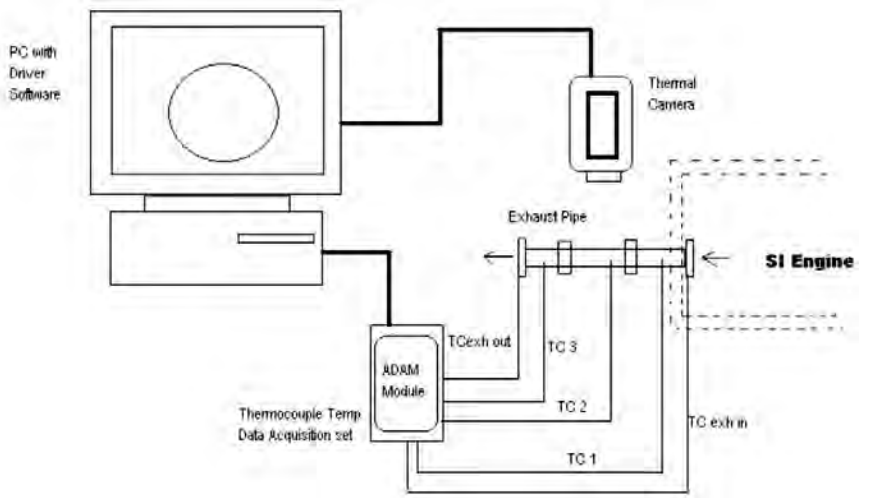

Figure 1. Schematic of experimental setup with thermal camera, DA module and exhaust pipe.

Table 1. Measured exhaust gas temperatures with different ID and average exhaust gas temperature

Load	T_{exh} IN	T_{exh} OUT	T_{exh1}	T_{exh} IN	T_{exh} OUT	T_{exh2}	T_{exh} IN	T_{exh} OUT	T_{exh3}	T_{exh3} Average
(W)	K (Exhaust ID = 25.0 mm)			K (Exhaust ID = 22.5 mm)			K (Exhaust ID = 20.0 mm)			(K)
0	375.348	372.76	374.054	376.217	373.086	374.652	376.802	373.199	375.001	374.568
200	498.634	494.198	496.416	498.982	494.249	496.616	499.017	494.381	496.699	496.576
400	541.413	538.483	539.948	542.017	538.503	540.26	542.194	538.725	540.46	540.222
600	579.921	574.53	577.226	579.983	574.697	577.34	580.103	574.815	577.459	577.341
800	590.552	587.247	588.9	590.614	588.023	589.319	590.791	588.116	589.454	589.223

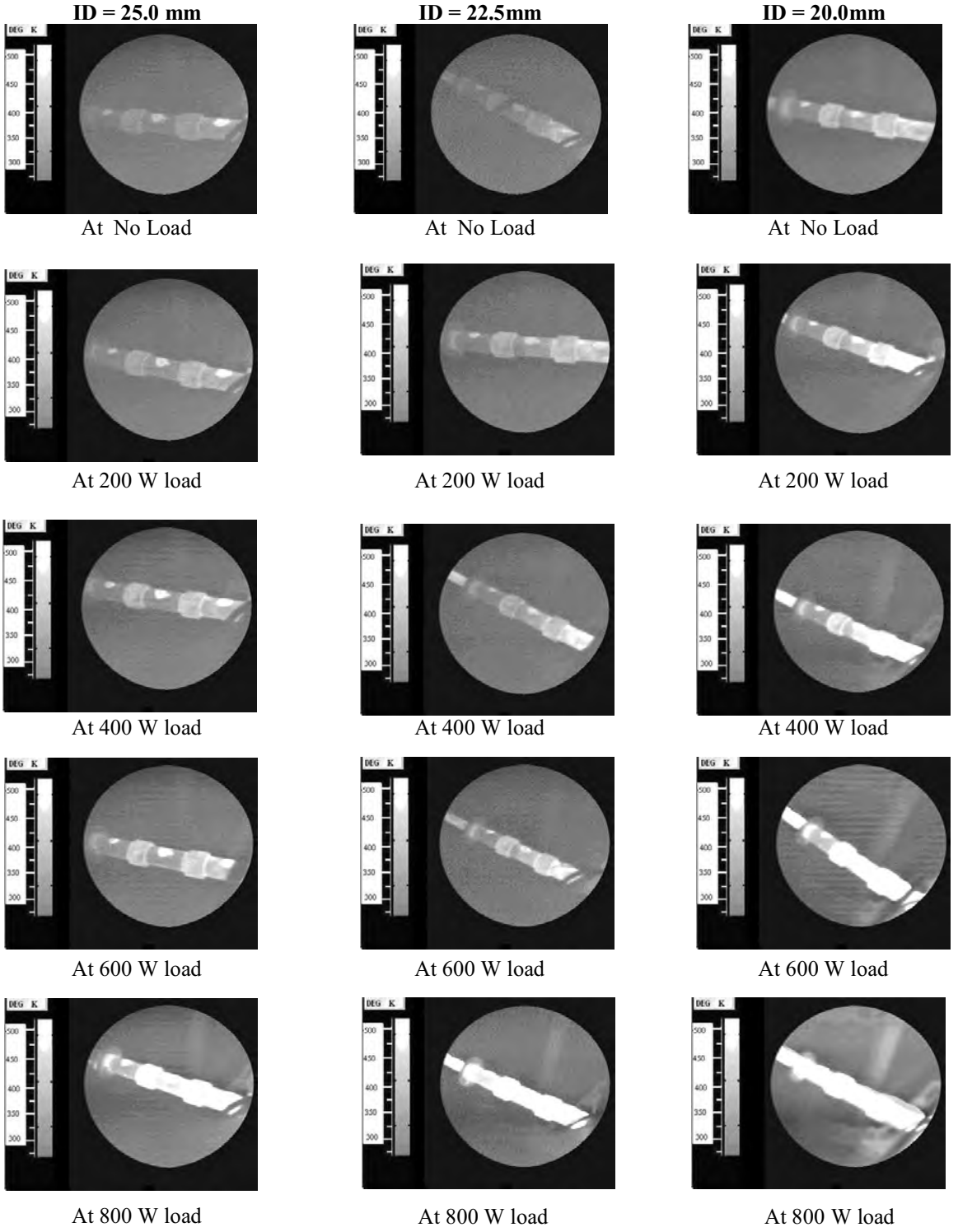

Figure 2. Thermographs of exhaust pipe for different flow areas at different loads.

4.1 Carbon Dioxide (CO_2) Properties Estimation

To estimate CO_2 properties at specified temperatures, an empirical relationship was used from the data[6] and a relationship was drawn using Microsoft Office Excel by regression analysis to derive the properties at various temperatures. The relationships for density, conductivity, viscosity, and Prandtl number are as follows:

$$\rho(kg/m^3) = 584.69\,(T)^{-1.0139} \quad (5)$$

$$k(W/m^0\mathrm{K}) = -2\times10^{-11}(T)^3 + 7\times10^{-8}(T)^2 + 4\times10^{-5}(T) - 0.0013 \quad (6)$$

$$\nu(m^2/S) = -3\times10^{-14}(T)^3 + 1\times10^{-10}(T)^2 + 3\times10^{-9}(T) - 6\times10^{-7} \quad (7)$$

$$\mathrm{P}r = 2.297(T)^{-0.1912} \quad (8)$$

Table 2. Exhaust flow rate measurements

Load (W)	Air flow m_{air} (kg/s)	Fuel flow m_{fuel} (kg/s)	Exhaust flow m_{exh} (kg/s)
0	0.0021748	0.0001625	0.00233727
200	0.0024313	0.0001885	0.00261979
400	0.0028251	0.0002079	0.00303300
600	0.0029279	0.0002340	0.00316190
800	0.0032622	0.0002925	0.00355470

The relationships have the accuracy of about 2 per cent. The results are tabulated in Table 3.

5. THERMAL RESISTANCE CALCULATIONS

For the experiment, a hollow cylinder of inner diameter 25 mm, thickness 6 mm, and length 300 mm was considered. It was assumed that the heat flows only in radial direction, so that the only space coordinate needed to specify the system is radius *r*. The surface temperature was evaluated for three different flow areas based on the analogy that reduction in area was due to excessive soot formation and the soot was evenly distributed along the inner surface of the exhaust pipe. In this experiment, two metallic tubes of thickness 1.25 mm in lieu of soot layer were used to give reduced flow area for the exhaust gas. Though, the thermal conductivity of the tubes was higher as compared to soot, the thermal resistance across the tubes, and subsequent temperature drop was very less and this difference can be ignored for the analysis.

- *For flow area with ID = 25.0 mm*

- *For flow area with ID = 22.5 mm*

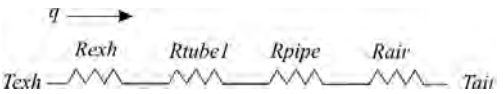

- *For flow area with ID = 20.0 mm*

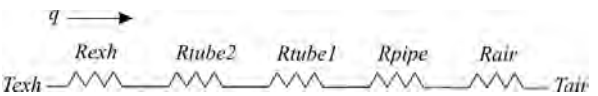

- *Heat transfer q is evaluated as*

$$q = \frac{T_{Exh} - T_{air}}{R_{total}}$$

where

$$R_{total} = R_{exh} + R_{pipe} + R_{air} \quad \text{(ID = 25.0 mm)}$$

$$= R_{exh} + R_{tube} + R_{pipe} + R_{air} \quad \text{(ID = 22.5 mm)}$$

$$= R_{exh} + R_{tube2} + R_{tube1} + R_{pipe} + R_{air} \quad \text{(ID = 20.0 mm)}$$

- *Convection resistance inside* R_{exh}

$$R_{exh} = \frac{1}{h_{exh} A} \tag{9}$$

where, h_{exh} = Exhaust convection coefficient (W/m^2 K), A = area (2 ð L) = 0.02356 m^2 (for ID 25.0 mm), = 0.02120 m^2 (for ID 22.5 mm), and = 0.01884 m^2 (for ID 20.0 mm).

$$h_{exh} = Nu \frac{k}{D} \tag{10}$$

where, Nu= Nusselt number, k = Thermal conductivity (W/m K), D = inner diameter (m)

$$\mathrm{N}u = (0.023)\,\mathrm{Re}^{0.8}\,\mathrm{P}r^{0.3} \tag{11}$$

where, R_e = Reynolds number, Pr = Prandtl number i.e.

$$\mathrm{R_e}\,\frac{vD}{v} \tag{12}$$

where, v = Kinematic viscosity (m^2/s), V = Flow velocity (m/s) i.e.

$$V = (m_{exh}) / (\rho_{exh} \times Flow\ area) \tag{13}$$

where, ρ_{exh} = CO_2 density (kg/m^3) and flow area = 0.0004908 m^2 (for ID = 25.0 mm), 0.0003976 m^2 (for ID = 22.5 mm), 0.0003141 m^2 (for ID = 20.0 mm).

Using the above relations, the various values of velocity, Reynolds number, Nusselt number and convection coefficient of exhaust for different flow areas at different loads are calculated.

- *Conduction resistance through Pipe* (R_{pipe})

$$R_{tube1} = \frac{1}{2\pi L k_{pipe}} ln(r_0 / r_i) = 0.00462\ (^{o}\mathrm{K/W}) \tag{14}$$

where, L = 0.3 (Pipe Length in m), k_{pipe} = 45 (Thermal conductivity , W/m ^{o}K), r_o = 0.0185 (outer radius in m), r_i = 0.0125 (inner radius in m).

Table 3. Interpolated properties of CO_2 at desired temperatures

Temp (K)	Density ρ (kg/m^3)	Conductivity k (W/m K)	Viscosity v (m^2/s)	Prandtl No (Pr)
374.568	1.4375	0.02245	0.000012977	0.739
496.516	1.0801	0.03337	0.000021875	0.701
540.222	0.9916	0.03758	0.000025474	0.689
577.341	0.9270	0.04127	0.000028691	0.681
589.223	0.9081	0.04248	0.000029748	0.678

- *Conduction resistance through Tube1* (R_{tube1})

$$R_{tube1} = \frac{1}{2\pi L k_{tube1}} ln(r_0 / r_i) = 0.001597\ (^oK/W) \quad (15)$$

where, L = 0.3 ; Pipe Length (m), k_{tube1} = 35 (Thermal conductivity , W/m ^{o}K), r_o = 0.0125 (outer radius, m), r_i = 0.01125 (inner radius, m). When soot conductivity k_{soot} = 24 W/m ^{o}K[7] then R_{soot1} = 0.002328 ^{o}K/W and the difference is 0.0007319 ^{o}K/W which can be neglected.

- *Conduction resistance through Tube2* (R_{tube2})

$$R_{tube1} = \frac{1}{2\pi L k_{tube2}} ln(r_0 / r_i) = 0.00178\ (^oK/W) \quad (16)$$

where, L= 0.3 (Pipe Length, m), k_{tube2} = 35 (Thermal conductivity, W/m ^{o}K), r_o = 0.01125 (outer radius , m), r_i = 0.01 (inner radius, m), When soot conductivity is k_{soot} = 24 W/m ^{o}K[7] then R_{soot2} = 0.002603 ^{o}K/W and the difference is 0.000823 ^{o}K/W which can be neglected.

- *Convection resistance outside* (R_{air})

$$Rair = \frac{1}{2\pi L r_0 h_{air}} = 1.147\ (^oK/W) \quad (17)$$

where, h_{air} = 25 (air convection coefficient, W/ m^2 ^{o}K)[8], r_o = 0.0185 (outer radius, m), L = 0.3 (pipe length, m).

Using the above relations, the various values of R_{exh} and R_{total} for different flow areas at different loads received are tabulated in Table 4.

- *Surface temperature calculation* (T_{surf})

The exhaust pipe surface temperature is calculated using following relation:

$$T_{surf} = T_{exh} - (\Delta T_{exh} + \Delta T_{pipe})$$

(ID = 25.0mm)

$$= T_{exh} - (\Delta T_{exh} + \Delta T_{tube1} + \Delta T_{pipe})$$

(ID = 22.5mm)

$$= T_{exh} - (\Delta T_{exh} + \Delta T_{tube1} + \Delta T_{tube2} + \Delta T_{pipe})$$

(ID = 20.0mm)

Using relationships

$\Delta T = T_{total} - T_{air}$

$Q = \Delta T / R_{total}$,

The temperature drop across pipe of different diameters was calculated for evaluation of T_{surf}. The surface temperature of the pipe is evaluated using thermocouples and IR temperature gun at different points and then an average value is considered for comparison with the measured surface temperature and the results have been tabulated in Table 5.

6. RESULTS

The differences in surface temperatures as evaluated by heat transfer analysis, IR thermometer and thermocouple at different loads with different IDs have been shown in Figs. 3-5. The surface temperatures analyzed differs slightly from the ones obtained by thermocouple and infrared thermometer, which could be attributed to the various assumptions relating to properties of exhaust gas. The temperatures evaluated directly by IR thermometer and thermocouple show consistency within a small range of

Table 4. Thermal resistance evaluations

Load (W)	Thermal resistance (^{o}K/W) for ID of 25.0 mm		Thermal resistance (^{o}K/W) for ID of 22.5 mm		Thermal resistance (^{o}K/W) for ID of 20.0 mm	
	$R_{exhaust}$	R_{total}	$R_{exhaust}$	R_{total}	$R_{exhaust}$	R_{total}
0	2.033	3.18462	1.869	3.022217	1.701	2.855997
200	1.5327	2.68432	1.4039	2.557117	1.282	2.436997
400	1.2839	2.43552	1.18	2.333217	1.0738	2.228797
600	1.18	2.33162	1.0871	2.240317	0.989	2.143997
800	1.0606	2.21222	0.975	2.128217	0.8872	2.042197

Table 5. Temperature evaluated for different IDs

Load (W)	Surface temp (^{o}K)			Thermocouple temp (^{o}K)			IR Temp (^{o}K)		
	Surface 25.0 mm	Surface 22.5 mm	Surface 20.0 mm	Surface 25.0 mm	Surface 22.5 mm	Surface 20.0 mm	Surface 25.0 mm	Surface 22.5 mm	Surface 20.0 mm
0	323.657	325.197	326.955	328.056	338.217	343.071	332.0	341.0	345.0
200	381.132	385.417	389.874	388.035	399.642	409.526	392.0	407.0	413.0
400	410.486	415.550	421.197	421.34	432.217	444.285	427.0	435.0	448.0
600	433.892	439.553	446.047	447.712	458.657	472.306	452.0	462.0	476.0
800	447.549	453.571	460.250	464.296	477.637	493.557	468.0	482.0	494.0

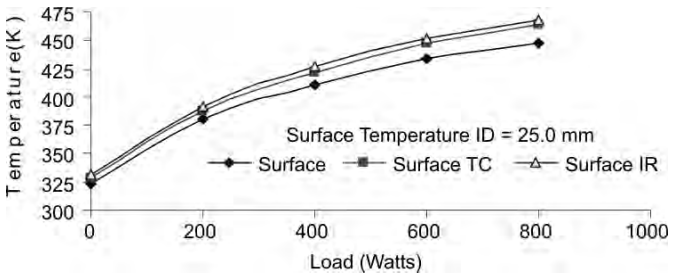

Figure 3. Differences in surface temperature for ID of 25.0 mm.

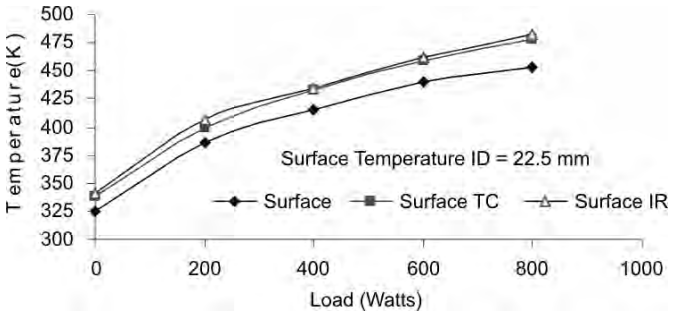

Figure 4. Differences in surface temperature for ID of 22.5 mm.

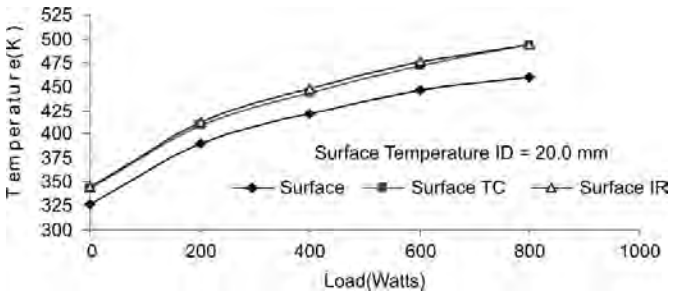

Figure 5. Differences in surface temperature for ID of 20.0 mm.

values. By taking the surface temperature values as obtained by thermocouples, it can be estimated that at higher loading of 800 W for the given engine, there exists a temperature increase of approximately 12 ^{o}K per mm of soot formation. The temperature rise is mainly due to the reduction in flow area as analysed using the properties of CO_2.

7. CONCLUSIONS

The thermographs of reduced flow area are brighter at corresponding loads as reduced area decreases high temperature heat transfer coefficient, the resistance of soot layer increases with increase in thickness. Hence an analogy can be drawn that the excessive soot formation (which can be further attributed to different engine running conditions) leads to reduced flow area and the same can be interpreted with the increase in temperature on the outer surface exhaust pipe. By taking the surface temperature values as obtained by thermocouples, it can be estimated that at higher loading of 800 W for the given engine, there exists a temperature increase of approximately 12 ^{o}K per mm of soot formation. The temperature rise is mainly due to the reduction in flow area as analyzed using the properties of CO_2. The thermal imaging at specified interval of engine running hours can be effectively used to see the variation in surface thermal pattern at prescribed load and at prescribed point and a general impression about the running of engine can be estimated.

ACKNOWLEDGEMENT

Authors are thankful to Vice-Chancellor, Defence Institute of Advanced Technology (Deemed University), Girinagar, Pune- 411025 for granting permission to publish this work.

REFERENCES

1. Hung-Yi, L.; Chao, S.M. & Tsai, G.L. Thermal performance measurement of heat sinks with confined impinging jet by infrared thermography. *Int. J. Heat Mass Transf.* 2005, **48**, 5386-394.
2. Centre for Power Efficiency and Environmental Protection Performance Optimiser No.: PO-EF-1001, CENPEEP, NTPC India, 2000.
3. Laskar, J.M.; Bagarvathiappan, S.; Sardar, M.; Jayakumar, T.; Philip, J. & Raj Baldev. Measurement of thermal diffusivity of solids using infrared thermography. *Material Letters,* 2008, **62**, 2740-742.
4. Ay, H.; Jang, J.Y. & Yeh, J.N. Local heat transfer measurement of plate finned-tube heat exchangers by infrared thermography. *Int. J. Heat Mass Transf.,* 2002, **45**, 4069-078.
5. Pastor, R.R. Characterization of exhaust flow in the catalytic converter of a spark- ignition engine using infrared thermography, ITC 092 A, InfraMation, 2003. pp. 08-15.
6. Holman, J. P. Heat transfers. Ed. 9. Tata McGraw-Hill Publishing Co. Ltd, 2005. 48 p.
7. http://www.reade.com/products/9-carbon—graphite-graphene-materials/100-carbon-black-carbon-black-carbon-lampblack-acetylene-black-animal-bone-charcoal-lampblack-fullerene-tubes-carbon-soot-
8. Janna, W. S. Engineering heat transfer. Ed. 2, CRC Press, 2000. 7 p.

Contributors

Mr Shiv Shankar Singh, graduated from of National Defence Academy, Khadakwasla, Pune, and Naval College of Engineering, INS Shivaji, Lonavla. He has completed Advanced Marine Engineering Course and ME Mechanical (Marine Engineering) at Defence Institute of Advanced Technology, Girinagar, Pune. He has carried out Instructional duties at Centre of Marine Engineering Technology at INS Shivaji, Lonavla. He has been Marine Engineer officer onboard Indian Naval Ships and is presently serving at Naval Dockyard, Visakhapatnam.

Dr A.K. Singh obtained his MSc from Agra University, Agra, in 1986 and PhD from University of Rajasthan, Jaipur, in 1992. Presently working at Defence Institute of Advanced Technology (DIAT), Deemed University, Girimnagar, Pune. His expertise include thermal and rheological properties of nanofluids, design and development of instrumentation for measuring thermal properties, thermal imaging for NDT, piezoelectric sensors/actuators and gas detection. He has been awarded with *DRDO Laboratory Scientist of the Year Award 2005*, *DIAT Researcher of the Year Award 2008* and is life member of Instrumentation Society of India.